Simulation of fast magnetic reconnection

E. Alec Johnson and James Rossmanith
Department of Mathematics, UW-Madison
July 8, 2008

Physical motivation: Space weather

Broad goal: to model **space weather**.

- Earth bombarded with **solar wind**.
- Solar wind is generally deflected by Earth's magnetic field.
- Reconnection of magnetic field lines allows plasma to enter the region occupied by Earth's magnetic field lines and propagate to Earth's poles.

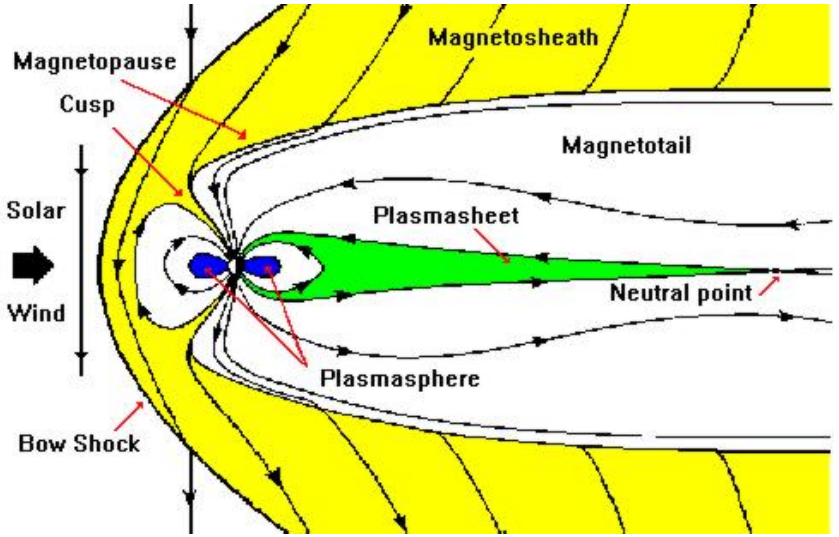

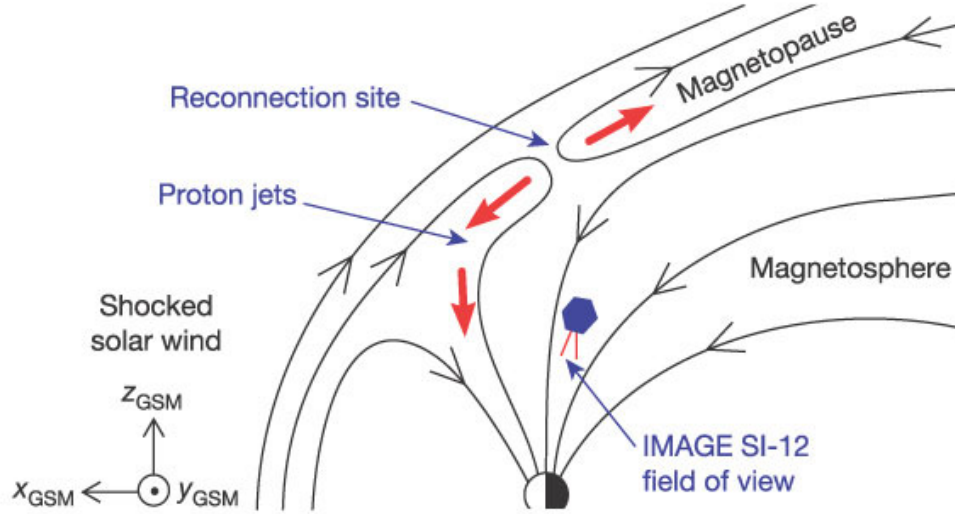

From *Continuous magnetic reconnection at Earth's magnetopause*,
H. U. Frey, T. D. Phan, S. A. Fuselier and S. B. Mende,
Nature 426, 533-537(4 December 2003)

Critical phenomenon: fast magnetic reconnection

Fast reconnection provides the mechanism that allows solar storms to trigger violent geomagnetic storms.

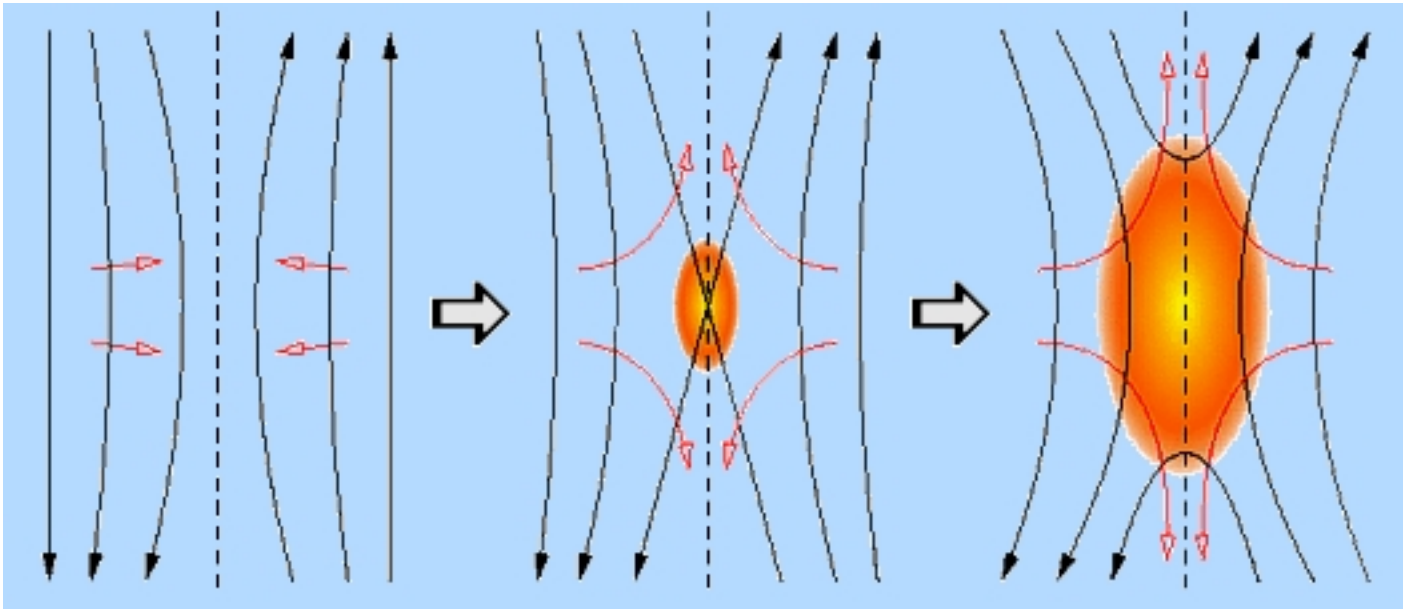

http://www.aldebaran.cz/astrofyzika/plazma/reconnection_en.html

Our project is to develop an efficient algorithm that resolves **fast magnetic reconnection**.

Simulating fast reconnection: a multiscale problem

Fast reconnection makes space weather a multiscale modeling problem. We seek the simplest (most computationally efficient) model that resolves the behavior of interest. Models that we have considered are

① Coarse model: **MHD** (magnetohydrodynamics)
- computationally cheap (does not admit fast waves)
- adequate for most of the domain
- ideal MHD does not admit reconnection
- resistive MHD does not admit fast reconnection

② Fine models (admit fast reconnection)

(a) Less Fine: **Hall MHD**
- admits fast (whistler) waves, but not light waves
- numerically difficult: differentiated source term with eigenvalues on the imaginary axis

(b) Fine: **2-fluid**
- pressure tensor
  i. **Maxwellian** (isotropic)
     – admits fast reconnection but structure of reconnection region is inaccurate
  ii. **Gaussian** (anisotropic)
     – agrees well with collisionless PIC

(c) Finest: Collisionless Kinetic (**PIC**: particle-in-cell)
- most computationally expensive; PIC is noisy
- gets right structure of reconnection region

For our choice of fine scale model, we are most interested in the Gaussian 2-fluid model, but so far have worked primarily with the Maxwellian 2-fluid model. We are implementing a PIC model as a standard of comparison.

Strategy: domain-decomposition

We want to develop a domain-decomposition multiscale algorithm which uses a kinetic model in small regions where reconnection is occurring and elsewhere uses MHD.

Why stitching models is a good idea:

- 2-fluid converges to MHD as gyroradius goes to zero
- ratio of explicit 2-fluid/PIC to MHD cost increases with inverse square of nondimensionalized gyroradius

Strategy for a stitched model. Framework of the domain-decomposition ("stitching") model we are working towards:

- use MHD solver over the global domain
- use embedded microscale (2-fluid/PIC) solver in regions where conditions are hospitable to fast reconnection

How data exchange should work:

- MHD provides microscale solver with boundary data
- microscale provides MHD with corrected values of state variables in overlap region.
- stitch smoothly at the boundary between models using a "sponge layer"

Model state variables

Exchanging data requires specifying the state variables of each model (and the maps between them.)

MHD (or Hall MHD) state variables:

$$\begin{pmatrix} \rho \\ \rho\mathbf{u} \\ \mathcal{E} \\ \mathbf{B} \end{pmatrix} = \begin{pmatrix} \text{mass} \\ \text{momentum} \\ \text{gas-dynamic energy} \\ \text{magnetic field} \end{pmatrix}$$

Maxwellian 2-fluid state variables:

$$\begin{pmatrix} \rho_i \\ \rho_i\mathbf{u}_i \\ \mathcal{E}_i \\ \rho_e \\ \rho_e\mathbf{u}_e \\ \mathcal{E}_e \\ \mathbf{B} \\ \mathbf{E} \end{pmatrix} = \begin{pmatrix} \text{ion mass} \\ \text{ion momentum} \\ \text{ion energy} \\ \text{electron mass} \\ \text{electron momentum} \\ \text{electron energy} \\ \text{magnetic field} \\ \text{electric field} \end{pmatrix}$$

PIC state variables:

$$\begin{pmatrix} \mathbf{B} \\ \mathbf{E} \\ (\mathbf{x}_p)_{p=1}^N \\ (\mathbf{v}_p)_{p=1}^N \end{pmatrix} = \begin{pmatrix} \text{magnetic field} \\ \text{electric field} \\ \text{particle positions} \\ \text{particle velocities} \end{pmatrix}$$

Gaussian 2-fluid state variables:

$$\begin{pmatrix} \rho_i \\ \rho_i\mathbf{u}_i \\ \mathbb{E}_i \\ \rho_e \\ \rho_e\mathbf{u}_e \\ \mathbb{E}_e \\ \mathbf{B} \\ \mathbf{E} \end{pmatrix} = \begin{pmatrix} \text{ion mass} \\ \text{ion momentum} \\ \text{ion energy tensor} \\ \text{electron mass} \\ \text{electron momentum} \\ \text{electron energy tensor} \\ \text{magnetic field} \\ \text{electric field} \end{pmatrix}$$

Mapping between micro and macro states

To traverse the hierarchy of models we need to specify mappings between state variables that are adjacent in the hierarchy.

- Mapping from micro to macro states is called *compression*.
- Mapping from macro to micro states is called *reconstruction*.
- Compression: typically involves straightforward summing or averaging
- Reconstruction: the inverse mapping is nonunique, so reconstruction requires additional assumptions or information to pick out a solution.

Mapping from Maxwellian 2-fluid to MHD states

An energy-conserving compression mapping from Maxwellian 2-fluid to MHD states is

$$\rho = \rho_i + \rho_e,$$
$$\rho\mathbf{u} = \rho_i\mathbf{u}_i + \rho_e\mathbf{u}_e,$$
$$\mathcal{E} = \mathcal{E}_i + \mathcal{E}_e \qquad \text{(problem!)}$$
$$\mathbf{B} = \mathbf{B}.$$

This mapping regards the drift velocity kinetic energy species drift velocity as part of the thermal energy in MHD. So the MHD gas-dynamic pressure computed by this mapping is $p_{\rm MHD} = p_i + p_e + \rho_i u_i^2/2 + \rho_e u_e^2/2$. The problem with this mapping is that the inverse mapping can compute negative species pressures even if the MHD pressure is positive, as we find in practice for strong shocks. Therefore we abandon energy conservation and instead assume that the MHD gas-dynamic pressure is the sum of the species pressures:

$$p_{\rm MHD} = p_i + p_e.$$

Reconstructing Maxwellian 2-fluid from MHD states

To invert the compression mapping we need additional information:

① *ratio of number densities*: provided by MHD assumption of quasineutrality:

$$\rho_i = \frac{m_i}{m_i + m_e}\rho, \qquad \rho_e = \frac{m_e}{m_i + m_e}\rho.$$

② *drift velocities*: provided by MHD assumptions of quasineutrality and $\partial_t \mathbf{E} \approx 0$ (Ampere's law):

$$\mathbf{J} = \mu_0^{-1} \nabla \times \mathbf{B},$$

$$\mathbf{u}_i = \mathbf{u} + \frac{m_e}{e\rho}\mathbf{J}, \qquad \mathbf{u}_e = \mathbf{u} - \frac{m_i}{e\rho}\mathbf{J}.$$

③ *ratio of thermal energies*: Would naturally use to split thermal energy. Instead, we split pressure to avoid negative pressures:

$$p_i = \frac{T_i}{T_i + T_e}p, \qquad p_e = \frac{T_e}{T_i + T_e}p$$

④ *Ohm's law*: Ohm's law is balance of net current solved for the electric field. Assuming quasineutrality gives:

$$\mathbf{E} = \eta\mathbf{J} + \mathbf{B}\times\mathbf{u} + \frac{\tilde{m}_i - \tilde{m}_e}{\rho}\mathbf{J}\times\mathbf{B} + \frac{1}{\rho}\nabla\cdot(\tilde{m}_e\mathbb{P}_i - \tilde{m}_i\mathbb{P}_e)$$
$$+ \frac{\tilde{m}_i\tilde{m}_e}{\rho}\Big(\partial_t\mathbf{J} + \nabla\cdot\big(\mathbf{uJ} + \mathbf{Ju} + \frac{\tilde{m}_e - \tilde{m}_i}{\rho}\mathbf{JJ}\big)\Big);$$

here $\tilde{m}_i := \frac{m_i}{e}$ and $\tilde{m}_e := \frac{m_e}{e}$ are species mass-to-charge ratios, and η is resistivity, which is assumed to be zero in the collisionless model. Ideal MHD uses a simplified Ohm's law which says that the electric field is zero in the reference frame of the fluid:

$$\mathbf{E} = \mathbf{B}\times\mathbf{u}.$$

Hall MHD also retains the Hall term, $\frac{\tilde{m}_i-\tilde{m}_e}{\rho}\mathbf{J}\times\mathbf{B}$. In the reconnection region we also expect the electron pressure term $\frac{\tilde{m}_i}{\rho}\nabla\cdot(\mathbb{P}_e)$ and the ion inertial term $\frac{\tilde{m}_i\tilde{m}_e}{\rho}\partial_t\mathbf{J}$ to be significant.

Mapping between Gaussian and Maxwellian 2-fluid states

The compression mapping from Gaussian to Maxwellian states is straightforward:

$$p_s = (1/3)\mathrm{trace}(\mathbb{P}_s).$$

(Recall that $\mathbb{E}_s = \mathbb{P}_s + \rho \mathbf{u}_s \mathbf{u}_s$; half the trace of this equation gives the isotropic constitutive relation $\mathcal{E}_s = (3/2)p + (1/2)\rho u^2$.)

The inverse mapping is provided by the assumption of isotropy:

$$\mathbb{P}_s = \begin{bmatrix} p & 0 & 0 \\ 0 & p & 0 \\ 0 & 0 & p \end{bmatrix}$$

Since the thermal energy is half the trace of the pressure tensor, these mappings conserve (thermal) energy.

Mapping between kinetic and 2-fluid states

① Compression mapping from kinetic to 2-fluid states:

- compute statistical moments for each cell to get values of mass, momentum, and pressure or energy.

② Reconstruction of particles from moments:

- uses moments and assumed form of distribution of velocities (e.g. Maxwellian or Gaussian)
- needed when creating particles for an initial state or injecting particles at model boundaries.

Equations: Vlasov

We take the Vlasov equation (i.e. the collisionless Boltzmann equation) as the true description of a collisionless plasma. It says that the particle density of each species is conserved in phase space.

$$\partial_t f_s + \nabla_{\mathbf{x}} \cdot (\mathbf{v} f_s) + \nabla_{\mathbf{v}} \cdot \left(\frac{q_s}{m_s} (\mathbf{E} + \mathbf{v} \times \mathbf{B}) f_s \right) = 0,$$

Here s is a species index, $f_s(t, \mathbf{x}, \mathbf{v})$ is particle density as a function of the independent variables.

Equations: kinetic

The equations of the kinetic model are Maxwell's equations and the Lorentz force to govern particle motion:

$$\partial_t \mathbf{B} = -\nabla \times E, \qquad \nabla \cdot \mathbf{B} = 0,$$

$$\partial_t \mathbf{E} = c^2 \nabla \times B - \mathbf{J}/\epsilon, \qquad \nabla \cdot \mathbf{E} = \sigma,$$

$$\partial_t (\gamma \mathbf{v}_p) = \frac{1}{r} \frac{q_p}{m_p} \Big(\mathbf{E}(\mathbf{x}_p) + \mathbf{v}_p \times \mathbf{B}(\mathbf{x}_p) \Big), \qquad \partial_t \mathbf{x}_p = \mathbf{v}_p,$$

$$\mathbf{J} = \sum_p q_p \mathbf{v}_p S,$$

where p denotes particle index and S denotes the spatial charge distribution of a single particle (e.g. an impulse function). (In the nondimensionalization r is the nondimensionalized gyroradius of a typical ion.)

Equations: 2-fluid

Two-fluid models use fluid equations to model the evolution of each species. The *collisionless* two-fluid model is obtained by taking moments of the Boltzmann equation,

$$\partial_t f_s + \nabla_{\mathbf{x}} \cdot (\mathbf{v} f_s) + \nabla_{\mathbf{v}} \cdot \left(\frac{q_s}{m_s} (\mathbf{E} + \mathbf{v} \times \mathbf{B}) f_s \right) = C_s,$$

where C_s is a collision operator. Assuming no interspecies collisions, mass and momentum evolution equations are

$$\partial_t \rho_s + \nabla \cdot (\rho_s \mathbf{u}_s) = 0,$$

$$\partial_t (\rho_s \mathbf{u}_s) + \nabla \cdot (\rho_s \mathbf{u}_s \mathbf{u}_s + \mathbb{P}_s) = \frac{q_s}{m_s} \rho_s (\mathbf{E} + \mathbf{u}_s \times \mathbf{B}),$$

where $s \in \{i, e\}$ denotes the ion or electron species, $\rho_s := m_s \int_{\mathbf{v}} f_s$ is the density, $\mathbf{u}_s := \langle v \rangle_s := \frac{\int_{\mathbf{v}} \mathbf{v} f_s}{\int_{\mathbf{v}} f_s}$ is the mean velocity, and $\mathbb{P}_s := \langle \mathbf{c}_s \mathbf{c}_s \rangle$ is the pressure tensor, where $\mathbf{c}_s := \mathbf{v} - \mathbf{u}_s$ is the thermal velocity. Note that there is no direct coupling between species. The two fluids interact only by means of their coupling to Maxwell's equations:

$$\begin{array}{rcccrcc} \partial_t \mathbf{B} + \nabla \times \mathbf{E} & = & 0, & & \nabla \cdot \mathbf{B} & = & 0, \\ \partial_t \mathbf{E} - c^2 \nabla \times \mathbf{B} & = & -(\sum_s \frac{q_s}{m_s} \rho_s \mathbf{u}_s)/\epsilon, & & \nabla \cdot \mathbf{E} & = & (\sum_s \frac{q_s}{m_s} \rho_s)/\epsilon. \end{array}$$

To close the system we need to specify the pressure tensor $\mathbb{P}_s$. Multiplying the Boltzmann equation by $\mathbf{cc}$ and integrating gives the pressure tensor evolution equation

$$\partial_t(\rho_s \mathbf{u}_s \mathbf{u}_s + \mathbb{P}_s) + \nabla \cdot \left(\rho_s \mathbf{u}_s \mathbf{u}_s \mathbf{u}_s + 3\,\mathrm{Sym}(\mathbf{u}_s \mathbb{P}_s) + \mathbb{P}_s^{[3]}\right)$$
$$= \frac{q_s}{m_s} 2\,\mathrm{Sym}\left(\rho_s \mathbf{u}_s \mathbf{E} + (\mathbb{P}_s + \rho_s \mathbf{u}_s \mathbf{u}_s) \times \mathbf{B}\right) + \int_{\mathbf{v}} \mathbf{c}_s \mathbf{c}_s C_s,$$

where Sym denotes the symmetric part of its argument tensor, $\mathbb{P}_s$ is the pressure tensor, and $\mathbb{P}_s^{[3]} := \rho \langle \mathbf{ccc} \rangle$ is the generalized heat flux.

The **ten-moment** two-fluid model neglects the collision term $\int {}_c\mathbf{cc}C_s$ and the generalized heat flux. The generalized heat flux vanishes if the distribution in velocity space is an aniostropic Gaussian, which we will assume.

The **ideal** two-fluid model instead uses the energy evolution equation (which is half the trace of the energy tensor evolution equation) and closes the system with the more restrictive assumption that the distribution in velocity space is Maxwellian. Again assuming no interspecies collisions,

$$\partial_t \left(\frac{1}{2}\rho_s u_s^2 + \frac{3}{2} p_s\right) + \nabla \cdot \left(\mathbf{u}_s \left(\frac{1}{2}\rho_s u_s^2 + \frac{3}{2} p_s\right) + \mathbf{u}_s p_s\right) = \frac{q_s}{m_s}(\rho_s \mathbf{u}_s \cdot \mathbf{E}).$$

We note that the Maxwellian 2-fluid model assumes equilibrating collisions and is inconsistent with the ten-moment model.

Equations: MHD

The equations of ideal MHD in conservative form are

$$\partial_t \begin{bmatrix} \rho \\ \rho\mathbf{u} \\ \tilde{\mathcal{E}} \\ \mathbf{B} \end{bmatrix} + \nabla \cdot \begin{bmatrix} \rho\mathbf{u} \\ \rho\mathbf{u}\mathbf{u} + \mathbb{I}\tilde{p}_{\mathrm{MHD}} - \mu_0^{-1}(\mathbf{B}\mathbf{B}) \\ \mathbf{u}(\tilde{\mathcal{E}} + \tilde{p}_{\mathrm{MHD}}) - \mu_0^{-1}\mathbf{B}\mathbf{B}\cdot\mathbf{u} \\ \mathbf{u}\mathbf{B} - \mathbf{B}\mathbf{u} \end{bmatrix} = 0,$$

where $\tilde{\mathcal{E}} = \mathcal{E} + \mu_0^{-1}B^2/2$ is total energy, where $\mathcal{E} = (3/2)p_{\mathrm{MHD}} + (1/2)\rho u^2$ is MHD gas energy, and $\tilde{p}_{\mathrm{MHD}} = p_{\mathrm{MHD}} + \mu_0^{-1}B^2/2$ is total pressure.

Numerical schemes

We have implemented second-order-accurate time-splitting shock-capturing schemes that maintain Maxwell's divergence constraints for the Ideal MHD and Maxwellian 2-fluid models in one and two dimensions of space.

(At this time my 1-D PIC code appears not to be conserving energy and my 1-D Gaussian 2-fluid code is giving non-positive-definite pressures.)

For the two-fluid solver, we used time-splitting to decouple the hyperbolic flux from the (nondifferentiated) source term. We used a shock-capturing method for the hyperbolic flux and RK4 for the source term ODE.

Numerical PIC scheme

Our PIC scheme will use staggering in time and space to achieve second-order accuracy and maintain the divergence constraints. (My current PIC code uses a finite-volume method for the electromagnetic field and appears to be losing energy.) Our scheme is:

$$(\partial_t \mathbf{E})^{m+1/2} = c^2 (\nabla \times B)^{m+1/2} - \mathbf{J}^{n+1/2}/\epsilon,$$

implicit case: $(\partial_t \mathbf{B})^{m+1/2} = -(\nabla \times E)^{m+1/2}$

explicit case: $(\partial_t \mathbf{B})^{m+1} = -(\nabla \times E)^{m+1}$

$$(\partial_t (\gamma \mathbf{v})_p)^n = \frac{1}{r}\frac{q_p}{m_p}\left(\mathbf{E}^n(\mathbf{x}_p^n) + \frac{\mathbf{v}_p^{n+1/2} + \mathbf{v}_p^{n-1/2}}{2} \times \mathbf{B}^n(\mathbf{x}_p^n)\right),$$

$$(\partial_t \mathbf{x}_p)^{n+1/2} = \mathbf{v}_p^{n+1/2}, \qquad \mathbf{J}^{n+1/2} = \sum_p q_p \mathbf{v}_p^{n+1/2} S.$$

For second-order accuracy we choose the particle shape S to be a mesh-cell-sized rectangle.

The discrete differential operators denote second-order centered difference operators in time and space. The spatial staggering (Yee scheme) centers vector components on the cell faces to which they are perpendicular and centers components of pseudovectors (e.g. $\mathbf{B}$) along cell edges. Taking the discrete divergence of the electromagnetic evolution equations shows that $\nabla \cdot \mathbf{B} = 0$ is maintained and that $(\nabla \cdot \mathbf{E})^n = \sigma^n/\epsilon$ is maintained if we enforce that current is charge flux, i.e., $(\partial_t \sigma)^{n+1/2} + \mathbf{J}^{n+1/2} = 0$.

2-D GEM study

James has implemented a 2D Discontinuous Galerkin shock-capturing solver for the Geospace Environmental Modeling Magnetic Reconnection Challenge Problem (**GEM reconnection problem**). Our two-fluid results replicate those of Hakim, Loverich, and Shumlak [Hakim06].

Boundary conditions. The domain is periodic in the x-axis. The boundaries perpendicular to the y-axis are conducting wall boundaries.

Initial conditions. The initial conditions are a perturbed Harris sheet equilibrium.

Model Parameters. We assumed that the ion to electron mass ratio was 25. For our nondimensionalization parameters we assumed that the gyroradius of the ions, the Debye length, and the light speed are all unity.

2-D GEM problem boundary conditions

Boundary conditions. A conducting wall boundary is a solid wall boundary (with slip boundary conditions in the case of ideal plasma) for the fluid variables, and the electric field at the boundary has no component parallel to the boundary. Assuming the Ideal MHD Ohm's law, this implies that at the conducting boundary the magnetic field must be parallel to the boundary.

So at the conducting wall boundaries

$$
\begin{aligned}
\partial_y \rho_s &= 0, \\
\partial_y u_{x,s} &= 0, \\
u_{y,s} &= 0, \\
\partial_y u_{z,s} &= 0,
\end{aligned}
$$

$$
\begin{aligned}
\partial_y B_{x,s} &= 0, \\
B_y &= 0, \\
\partial_y B_z &= 0, \\
E_x &= 0, \\
\partial_y E_y &= 0, \\
E_z &= 0.
\end{aligned}
$$

2-D GEM problem initial conditions

Initial conditions. The initial conditions are a perturbed Harris sheet equilibrium. The unperturbed equilibrium is given by

$$\begin{aligned}
\mathbf{B}(y) &= B_0 \tanh(y/\lambda)\mathbf{e}_x, \\
\mathbf{E} &= 0, \\
n_i(y) &= n_e(y) \\
&= n_0(1/5 + \operatorname{sech}^2(y/\lambda)), \\
p(y) &= \frac{B_0^2}{2n_0} n(y), \\
p_e(y) &= p(y)/6, \\
p_i(y) &= 5p(y)/6.
\end{aligned}$$

Following [Hakim06], we assumed that the initial current is carried only by the electrons:

$$\mathbf{J}_e = -\frac{B_0}{\lambda} \operatorname{sech}^2(y/\lambda).$$

On top of this the magnetic field is perturbed by

$$\delta\mathbf{B} = \mathbf{e}_z \times \nabla(\psi), \text{ where}$$

$$\psi(x,y) = \psi_0 \cos(2\pi x/L_x)\cos(\pi y/L_y);$$

here $[-L_x/2, L_x/2]\times[-L_y/2, L_y/2]$ is the computational domain. We chose the same parameter values as in [Hakim06],

$$\begin{aligned}
L_x &= 4\pi, & n_0 &= 1, \\
L_y &= 2\pi, & B_0 &= 0.1, \\
\lambda &= 0.5, & \psi_0 &= B_0/10.
\end{aligned}$$

In [Birn01] (the original GEM problem) $B_0 = 1$; to compare results we use $\mathbf{B} = .1\mathbf{B}_{\text{GEM}}$, $t = 10t_{\text{GEM}}$, $\mathbf{u} = .1\mathbf{u}_{\text{GEM}}$, $\mathbf{E} = .01\mathbf{E}_{\text{GEM}}$, $p = .01p_{\text{GEM}}$, $\mathcal{E} = .01\mathcal{E}_{\text{GEM}}$, etc.

Numerical parameters. We used a 512×256 mesh.

GEM reconnection challenge 2-fluid solution using DG

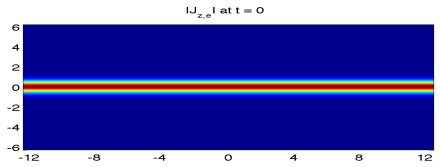

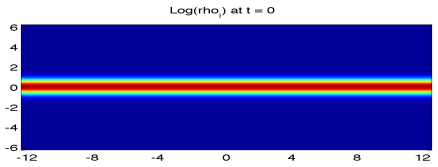

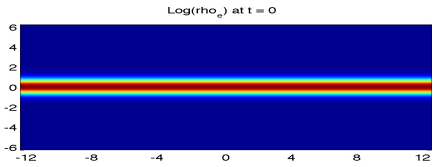

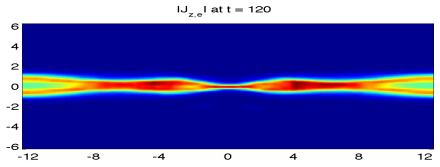

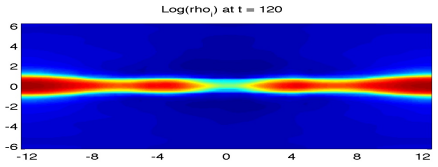

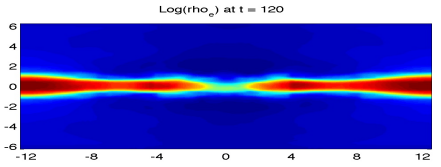

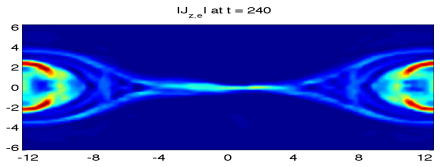

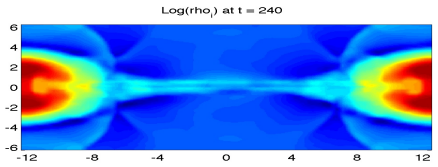

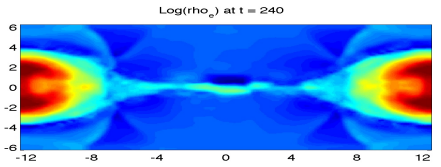

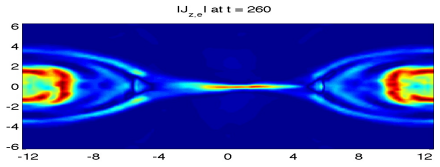

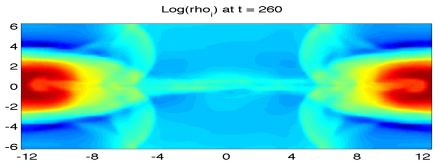

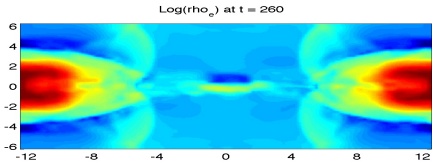

GEM reconnection challenge 2-fluid solution using DG: $|J_{z,e}|$ ——

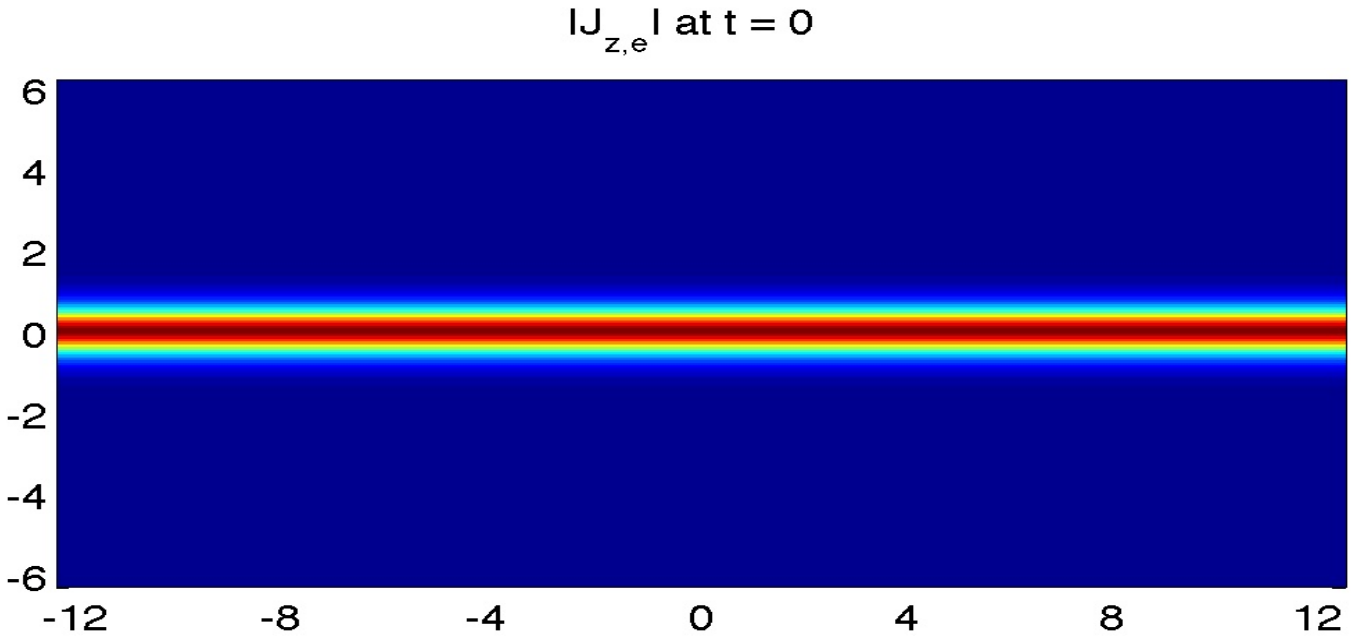

GEM reconnection challenge 2-fluid solution using DG: $|J_{z,e}|$

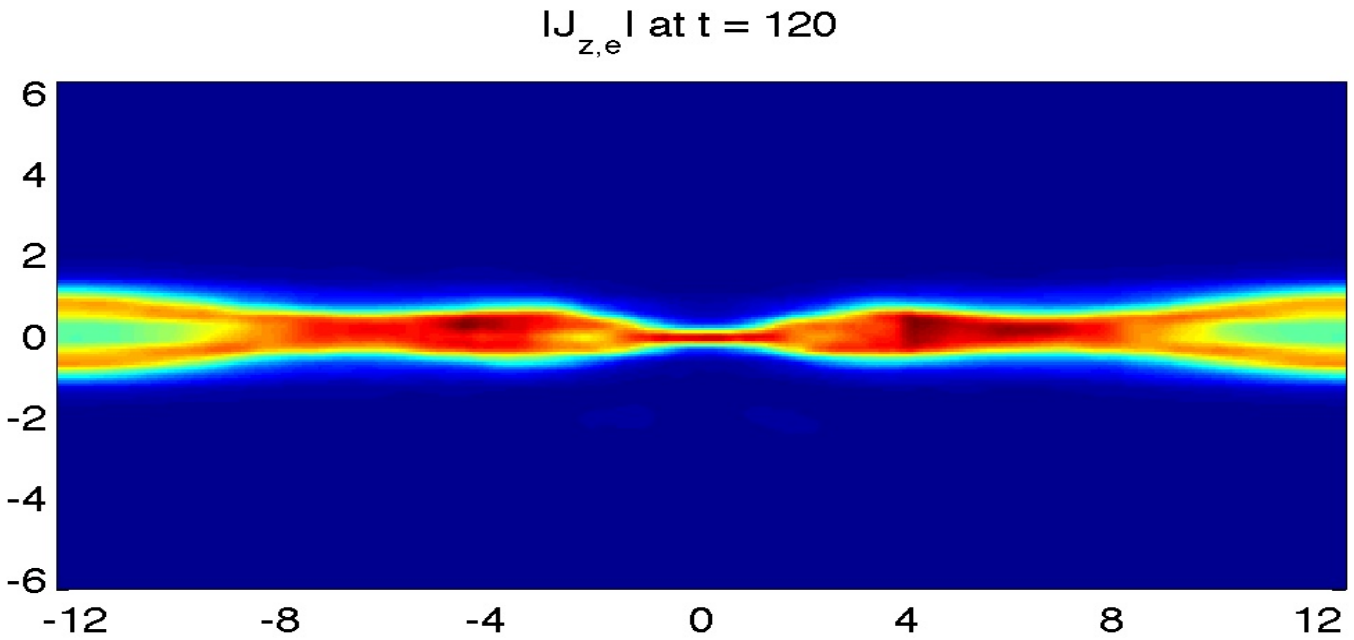

GEM reconnection challenge 2-fluid solution using DG: $|J_{z,e}|$

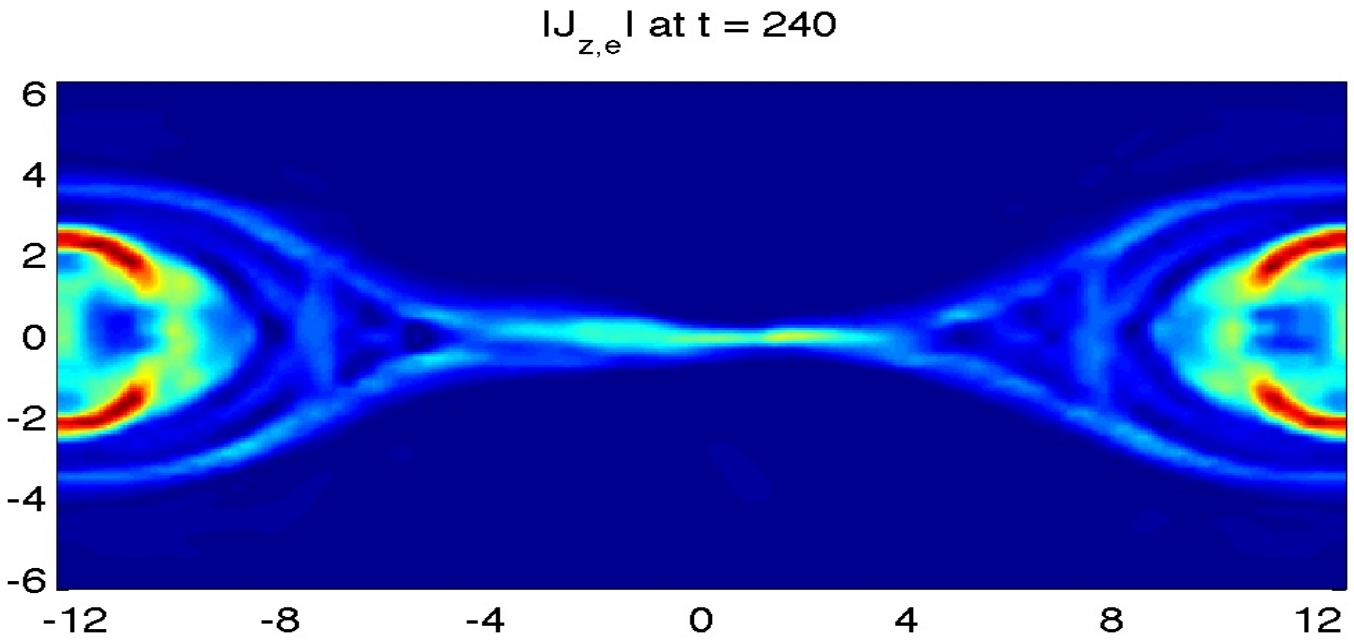

GEM reconnection challenge 2-fluid solution using DG: $|J_{z,e}|$

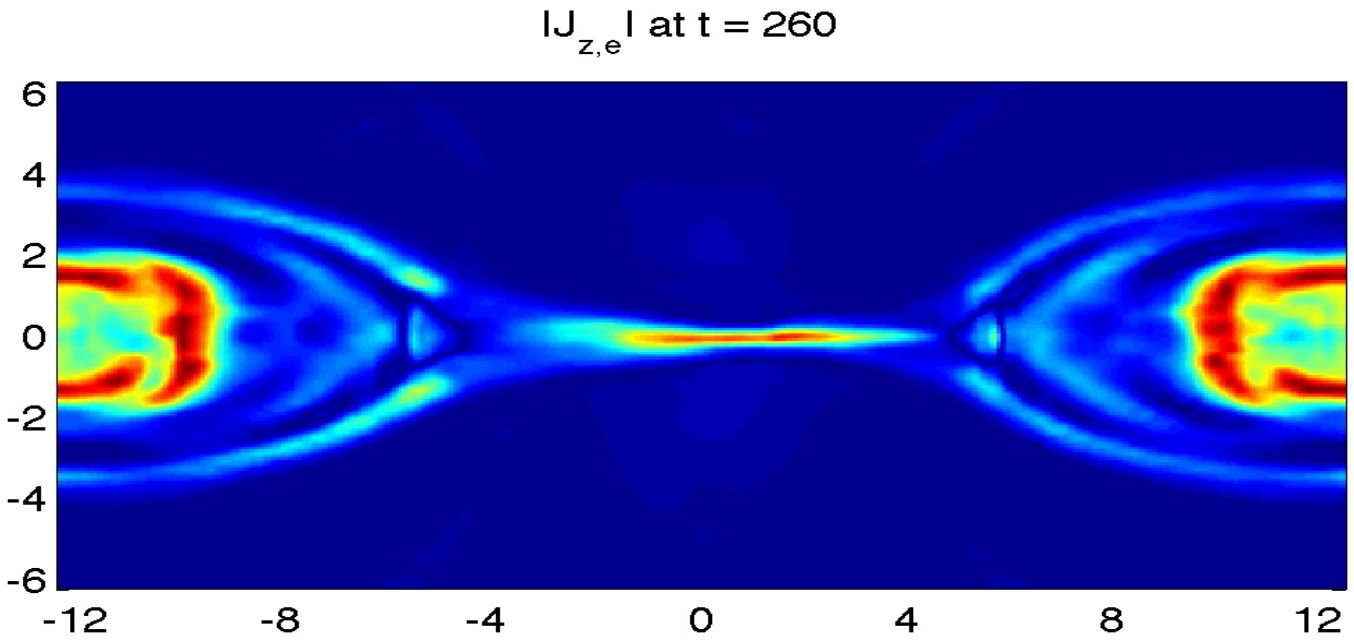

GEM reconnection challenge 2-fluid solution using DG: ρ_i

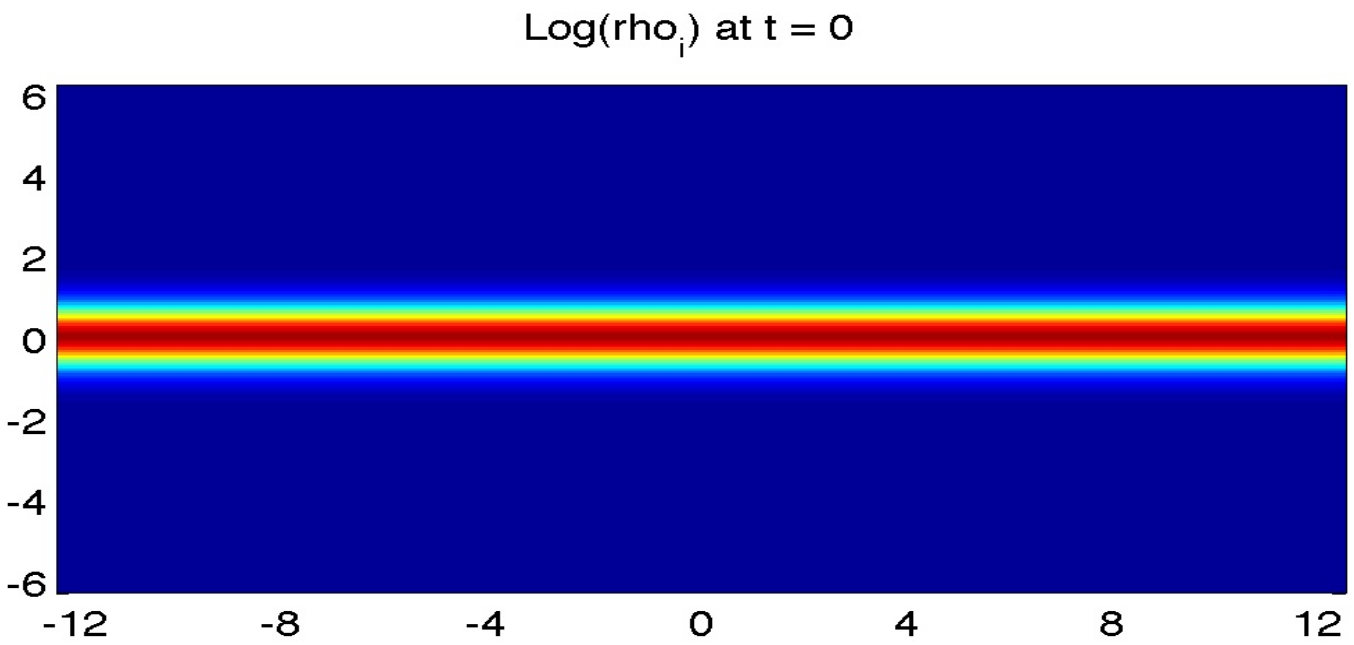

GEM reconnection challenge 2-fluid solution using DG: ρ_i

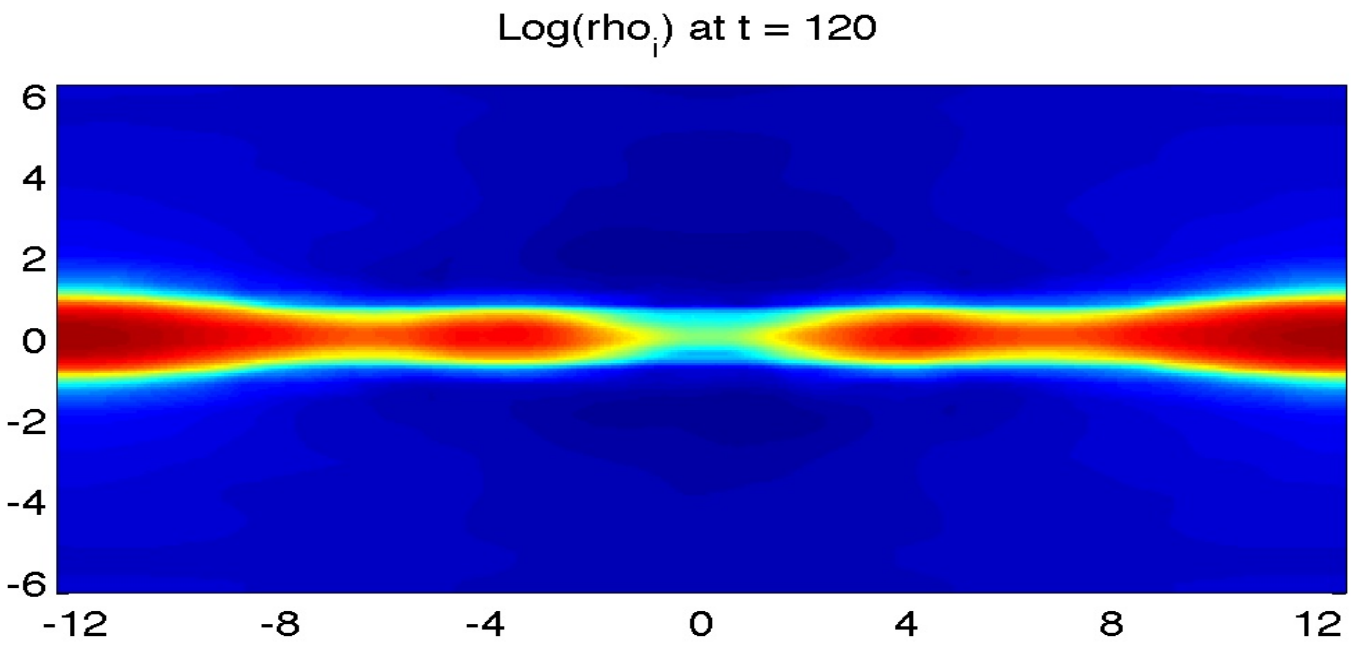

GEM reconnection challenge 2-fluid solution using DG: ρ_i

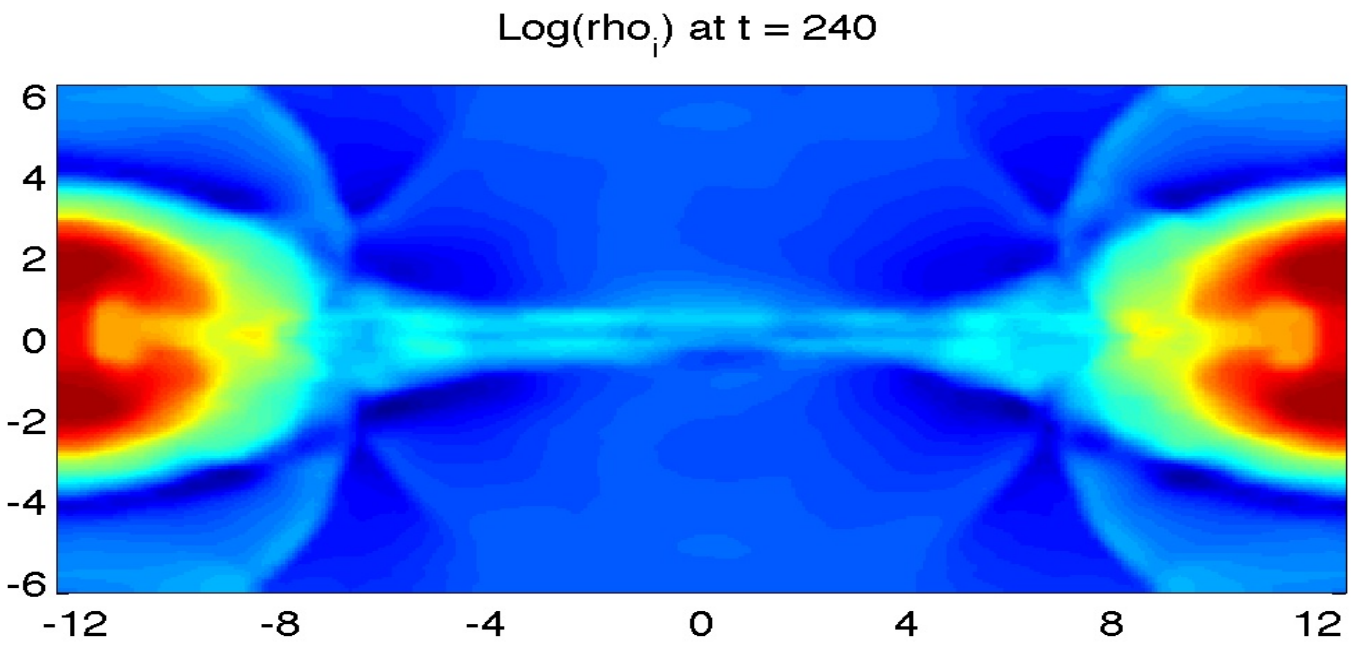

GEM reconnection challenge 2-fluid solution using DG: ρ_i

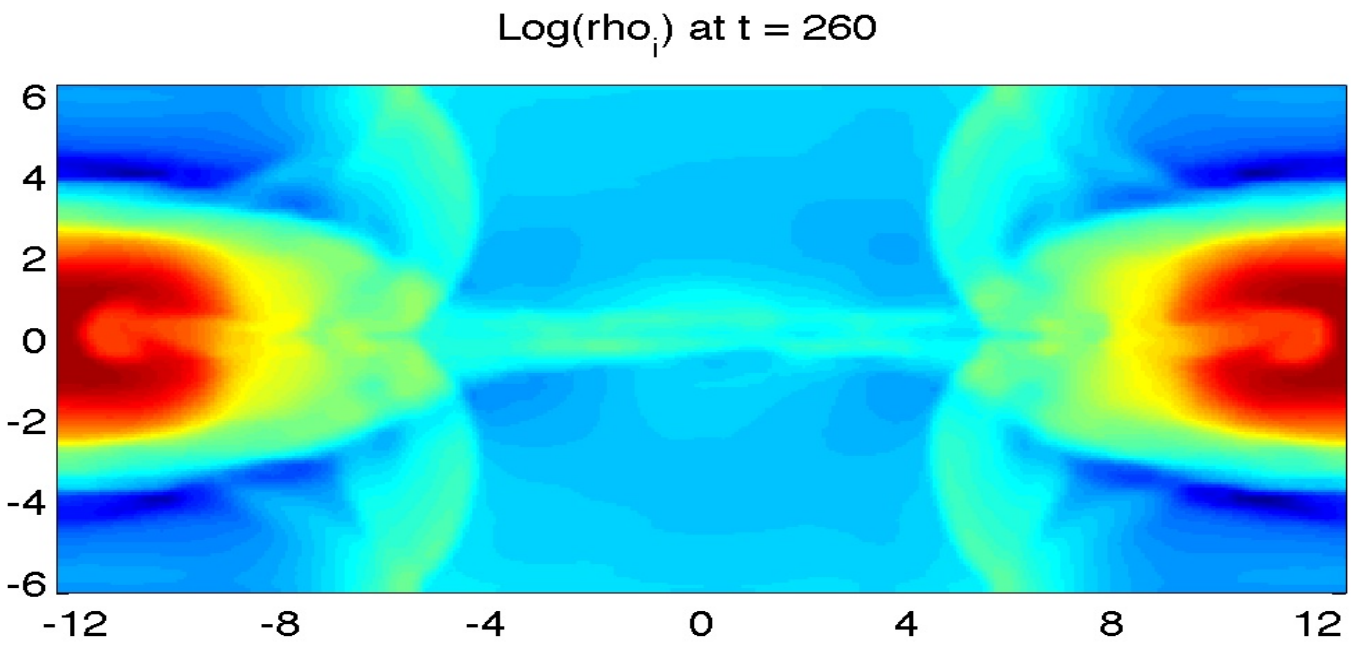

GEM reconnection challenge 2-fluid solution using DG: ρ_e

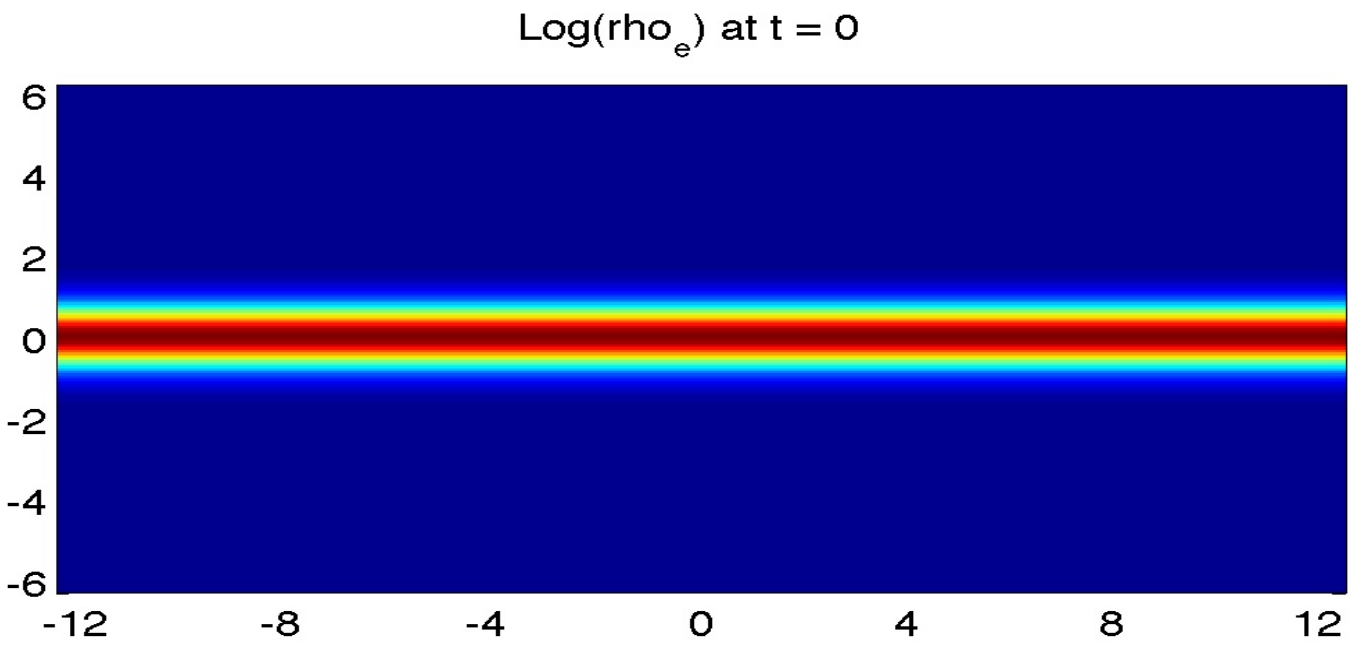

GEM reconnection challenge 2-fluid solution using DG: ρ_e

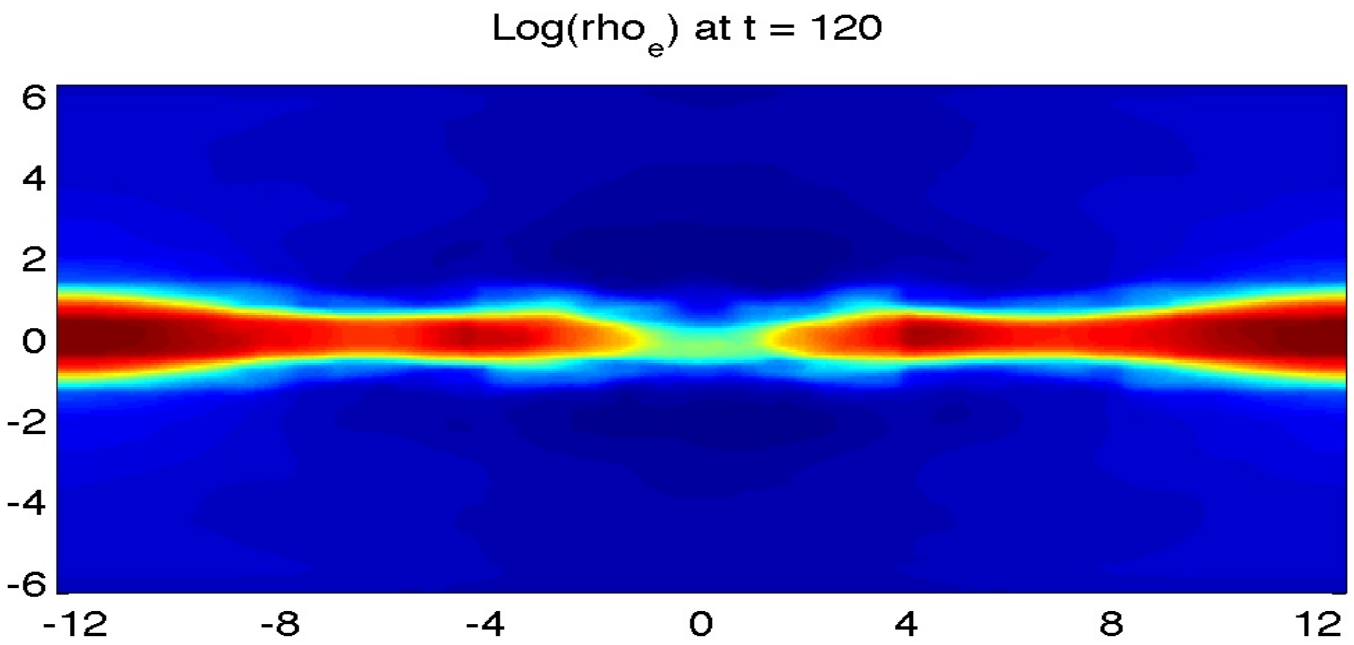

GEM reconnection challenge 2-fluid solution using DG: ρ_e

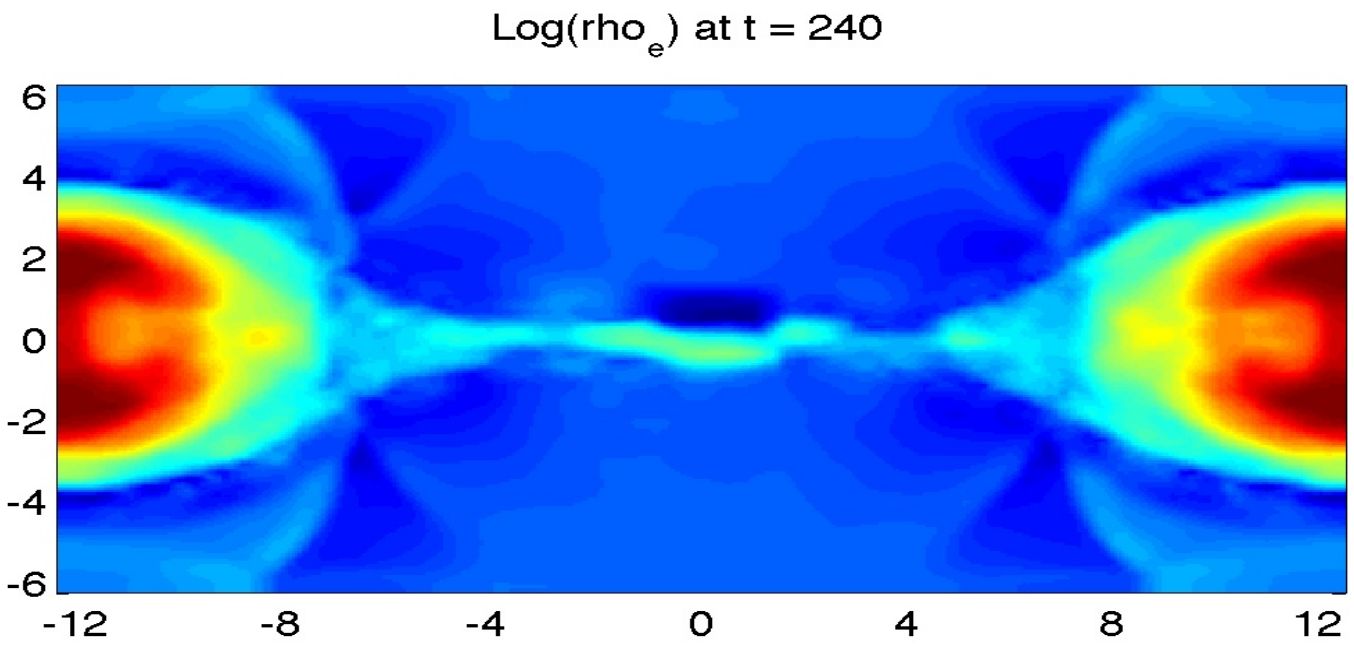

GEM reconnection challenge 2-fluid solution using DG: ρ_e

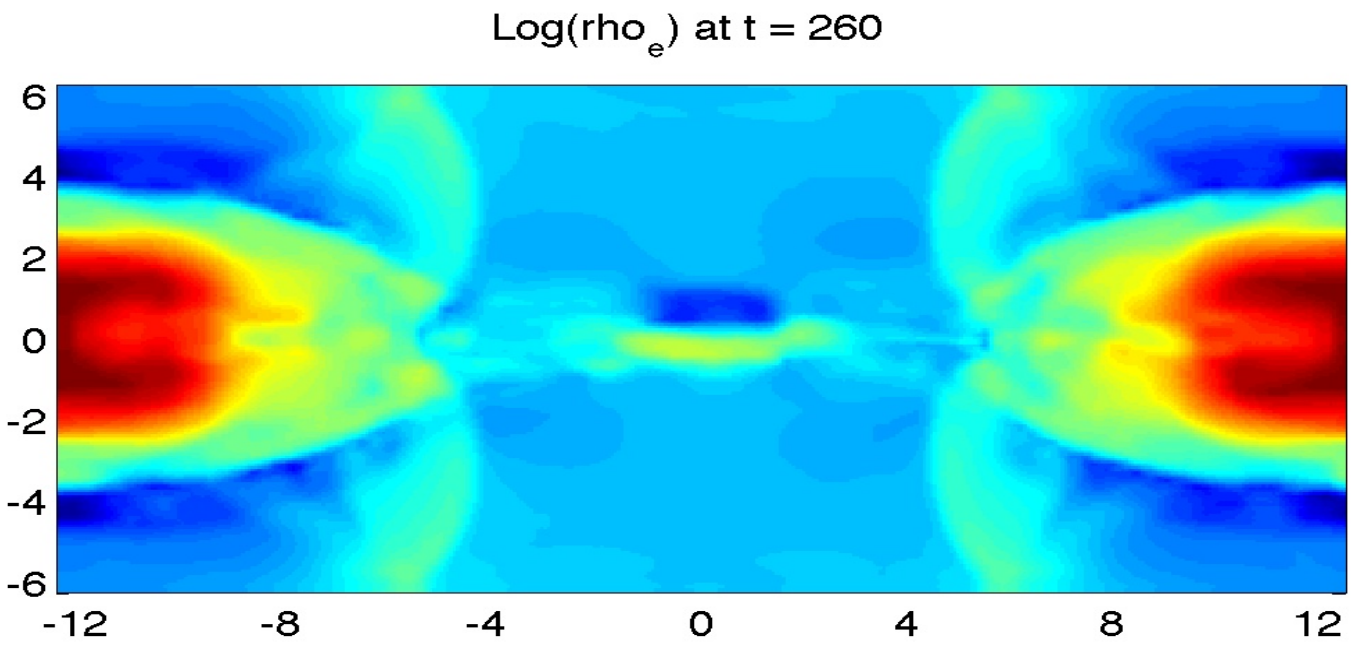

GEM 2-fluid DG solution: reconnected flux

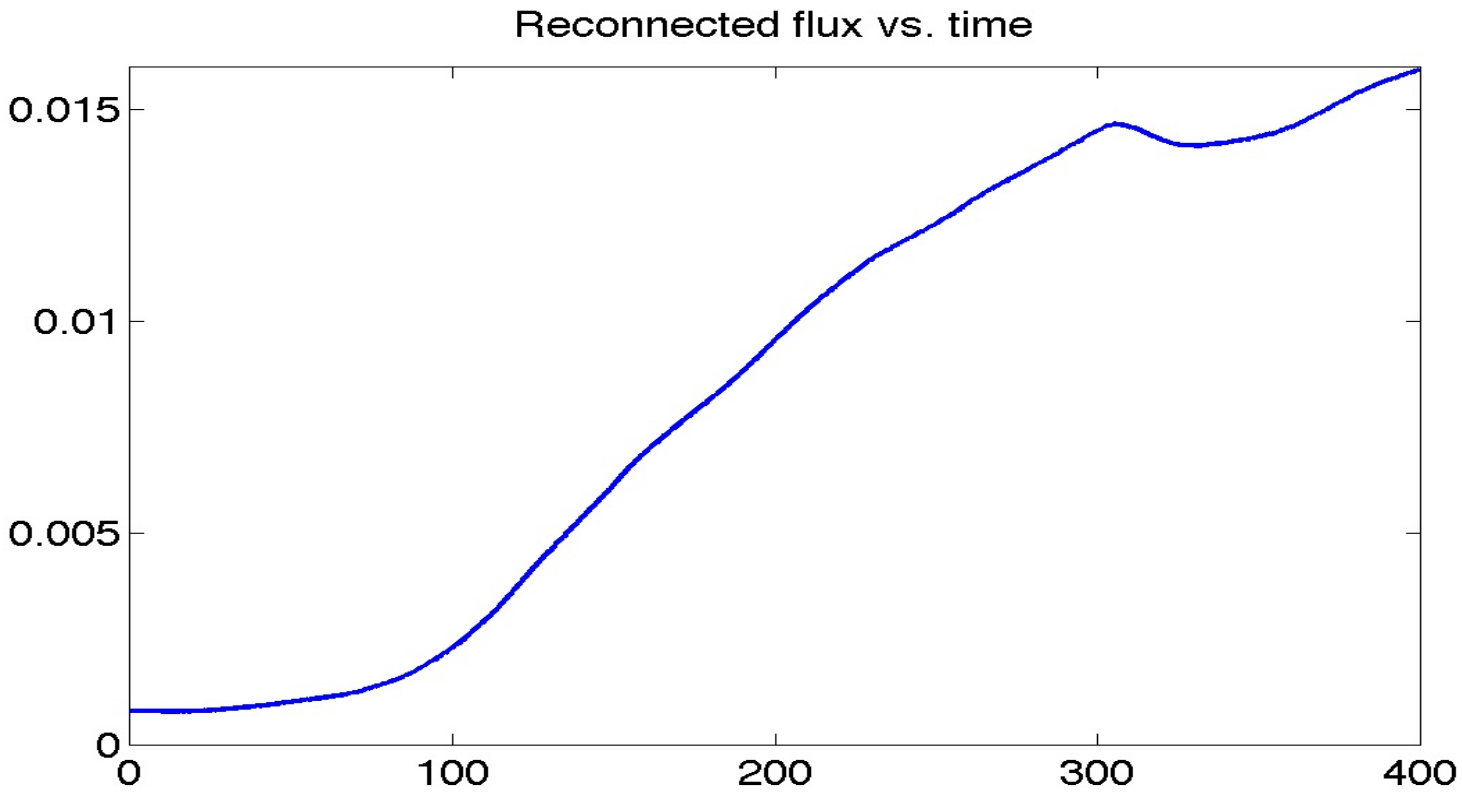

Preliminary 1D studies

The need to design a stitched model has prompted us to carry out some preliminary studies. We need to show that waves are transmitted smoothly across the stitching layer between model boundaries, and for this we need to study convergence of microscale model to macroscale model to determine where to use the macroscale versus microscale model.

We have done 1D convergence studies for the MHD, 2-fluid, and PIC models for the Brio-Wu shock problem, polarized Alfvèn waves, and Magnetosonic waves.

We find that (1) For a large light speed, as gyroradius goes to zero, the 2-fluid simulation seem to weakly converge to a limit that is close to the 1-fluid simulation, and (2) PIC simulations show rough agreement with 2-fluid simulations as we increase the number of particles.

Computations: Brio-Wu shock problem

For **MHD** the Brio-Wu initial conditions to the left and right of zero are:

$$\begin{bmatrix} \rho \\ v^1 \\ v^2 \\ v^3 \\ p \\ B^1 \\ B^2 \\ B^3 \end{bmatrix}_{\text{left}} = \begin{bmatrix} 1.0 \\ 0 \\ 0 \\ 0 \\ 1.0 \\ 0.75 \\ 1.0 \\ 0 \end{bmatrix} \quad \text{and} \quad \begin{bmatrix} \rho \\ v^1 \\ v^2 \\ v^3 \\ p \\ B^1 \\ B^2 \\ B^3 \end{bmatrix}_{\text{right}} = \begin{bmatrix} 0.125 \\ 0 \\ 0 \\ 0 \\ 0.1 \\ 0.75 \\ -1.0 \\ 0 \end{bmatrix}$$

Roughly equivalent **two-fluid** initial conditions are:

$$\begin{bmatrix} \rho_i \\ v_i^1 \\ v_i^2 \\ v_i^3 \\ p_i \\ \rho e \\ v_e^1 \\ v_e^2 \\ v_e^3 \\ pe \\ B^1 \\ B^2 \\ B^3 \\ E^1 \\ E^2 \\ E^3 \end{bmatrix}_{\text{left}} = \begin{bmatrix} 1.0 \\ 0 \\ 0 \\ 0 \\ 0.5 \\ 1.0\frac{me}{m_i} \\ 0 \\ 0 \\ 0 \\ 0.5 \\ 0.75 \\ 1.0 \\ 0 \\ 0 \\ 0 \\ 0 \end{bmatrix} \quad \text{and} \quad \begin{bmatrix} \rho_i \\ v_i^1 \\ v_i^2 \\ v_i^3 \\ p_i \\ \rho e \\ v_e^1 \\ v_e^2 \\ v_e^3 \\ pe \\ B^1 \\ B^2 \\ B^3 \\ E^1 \\ E^2 \\ E^3 \end{bmatrix}_{\text{right}} = \begin{bmatrix} 0.125 \\ 0 \\ 0 \\ 0 \\ 0.05 \\ 0.125\frac{me}{m_i} \\ 0 \\ 0 \\ 0 \\ 0.05 \\ 0.75 \\ -1.0 \\ 0 \\ 0 \\ 0 \\ 0 \end{bmatrix}$$

Computations

We plotted ion density at nondimensionalized time $t = 0.1$ for a range of values of the nondimensionalized Larmor radius:

- $r_L = \infty$ (an Euler gas dynamics computation),
- $r_L = 10, 1, 0.1, 0.01, 0.003$ (two-fluid computations), and
- $r_L = 0$ (an ideal MHD computation).

Results:

- As $r_L \longrightarrow 0$, the solution seems to weakly approach the MHD solution.
- For smaller values of r_L computation becomes prohibitively expensive as we need a finer computational grid to prevent negative pressures or densities from crashing the code and to get convergence.
- For intermediate values of r_L, the computational domain needs to be extended the most due to substantial fast-moving oscillations.

Computations (cell-centered), $r_L = 10$

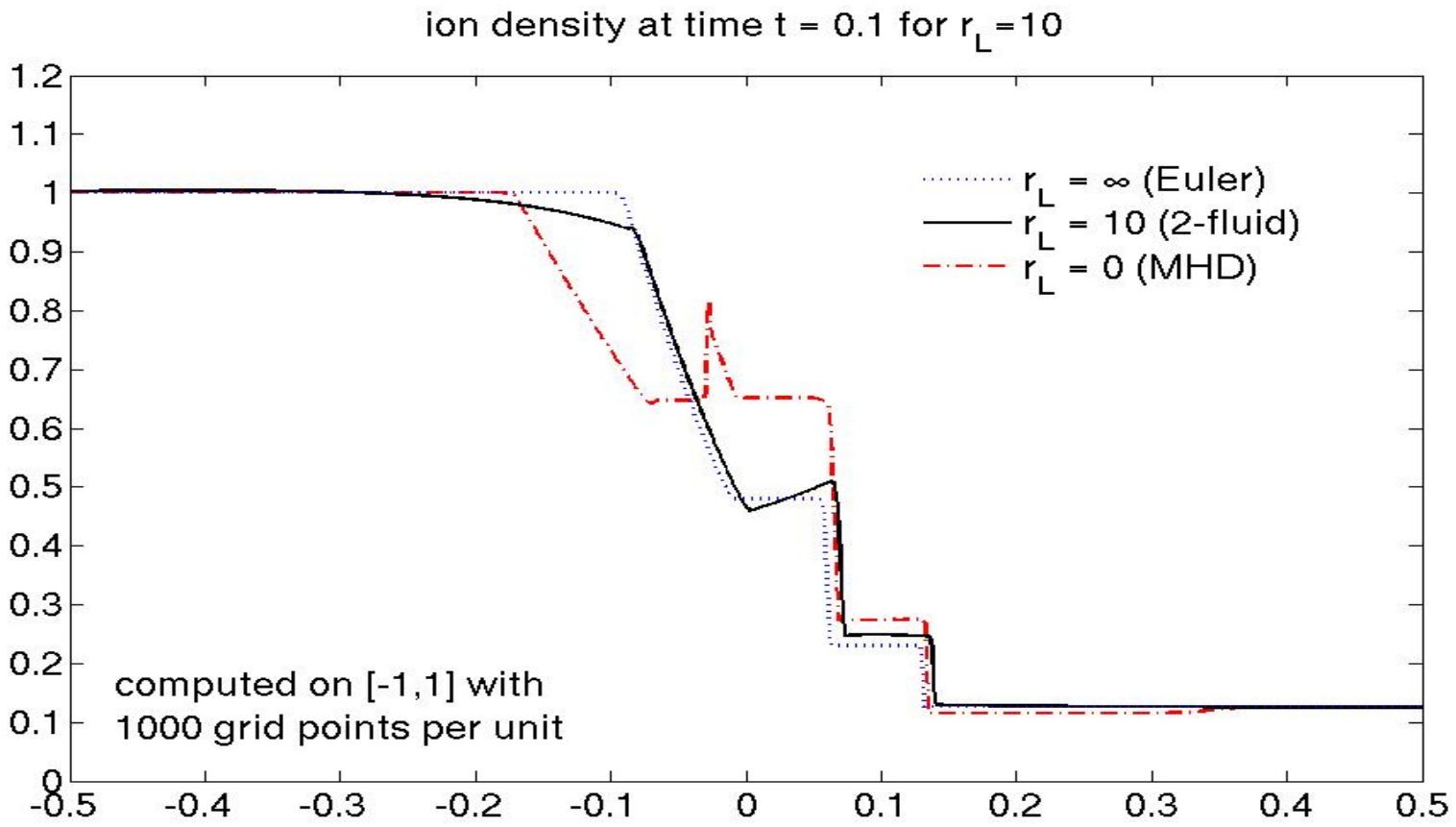

When the Larmor radius is large ($r_L = 10$), the electromagnetic effects are weak and the ions behave like an ideal gas. (At $r_L = 100$, 2-fluid is indistinguishable from Euler.)

Computations (cell-centered), $r_L = 1$

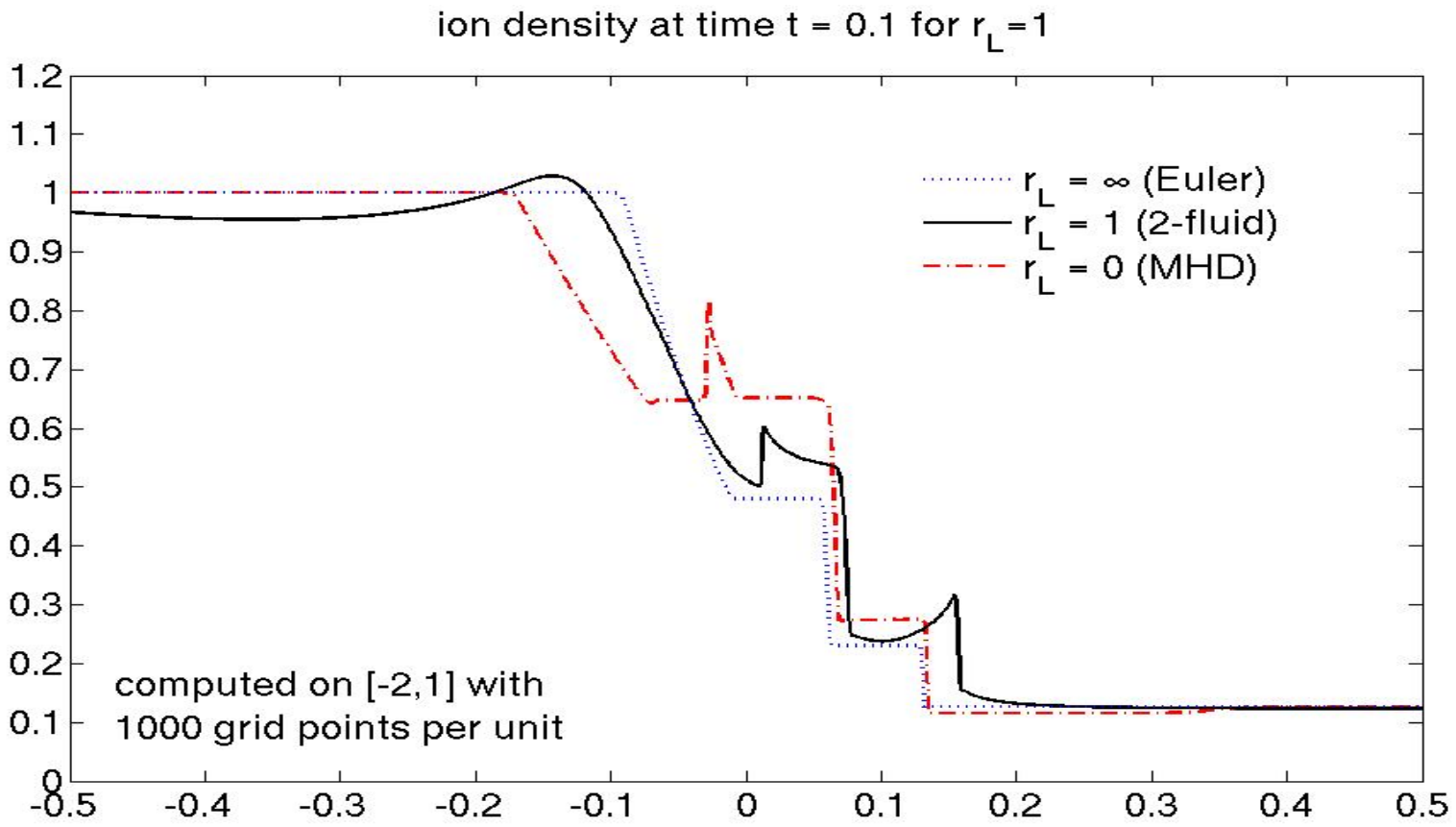

As we decrease the Larmor radius, the solution begins to transition away from gas dynamics (and eventually toward MHD).

Computations (cell-centered), $r_L = 0.1$

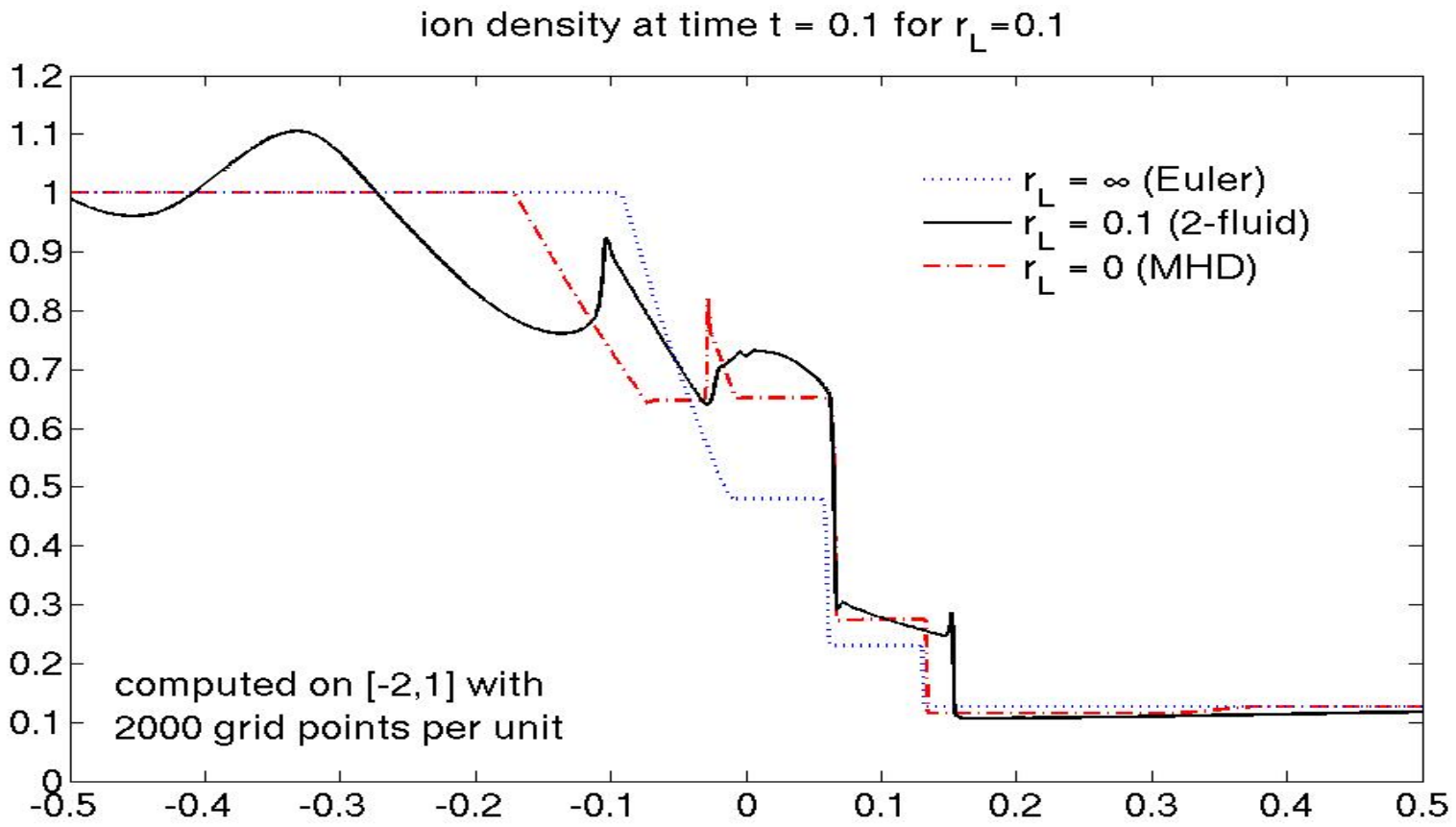

When $t \approx r_L$, the solution is roughly intermediate between Euler and MHD.

Computations (cell-centered), $r_L = 0.01$

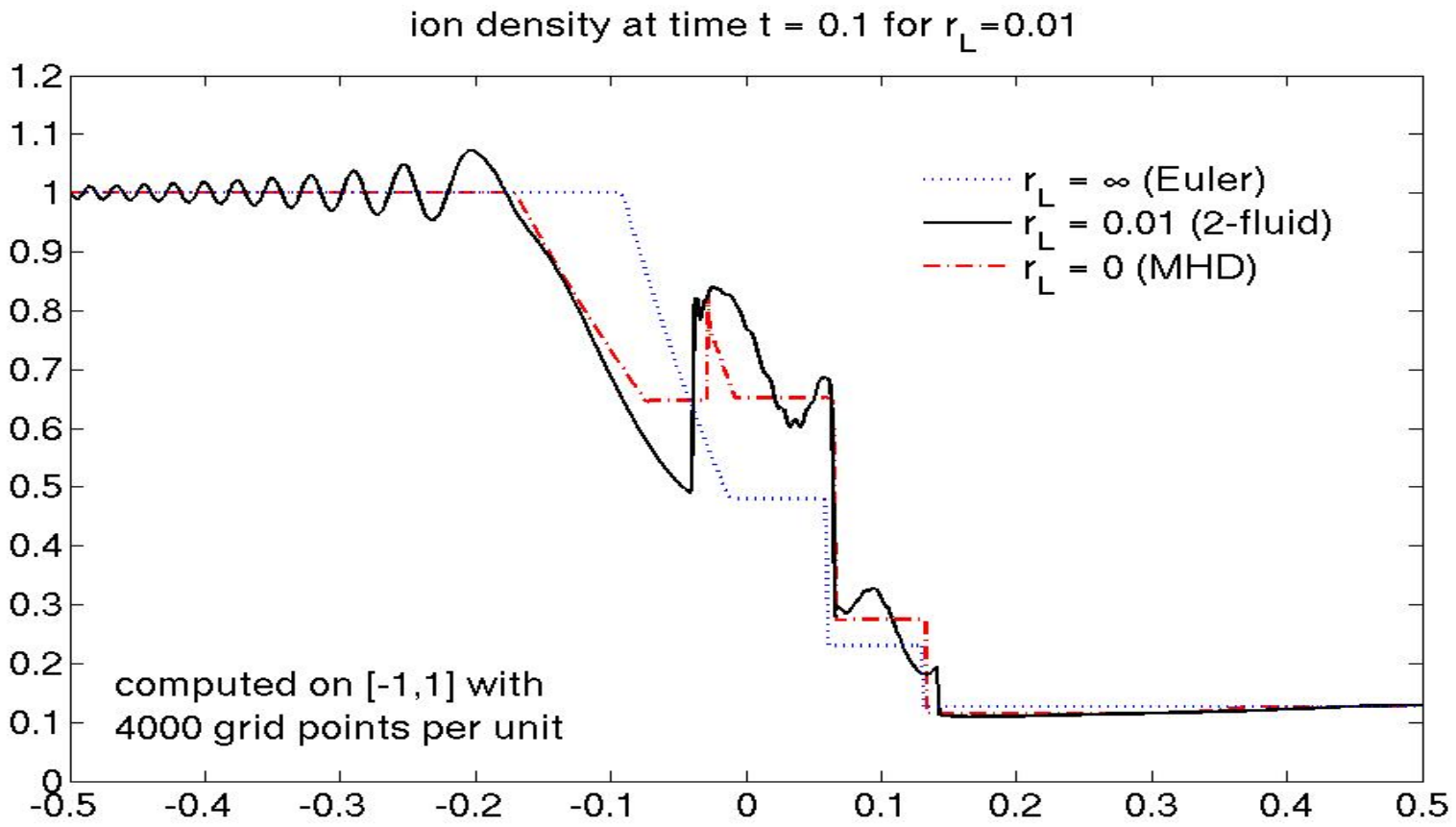

As the Larmor radius becomes even smaller, the frequency of the oscillations increases and the solution begins to weakly approach the MHD solution.

Computations (cell-centered), $r_L = 0.003$

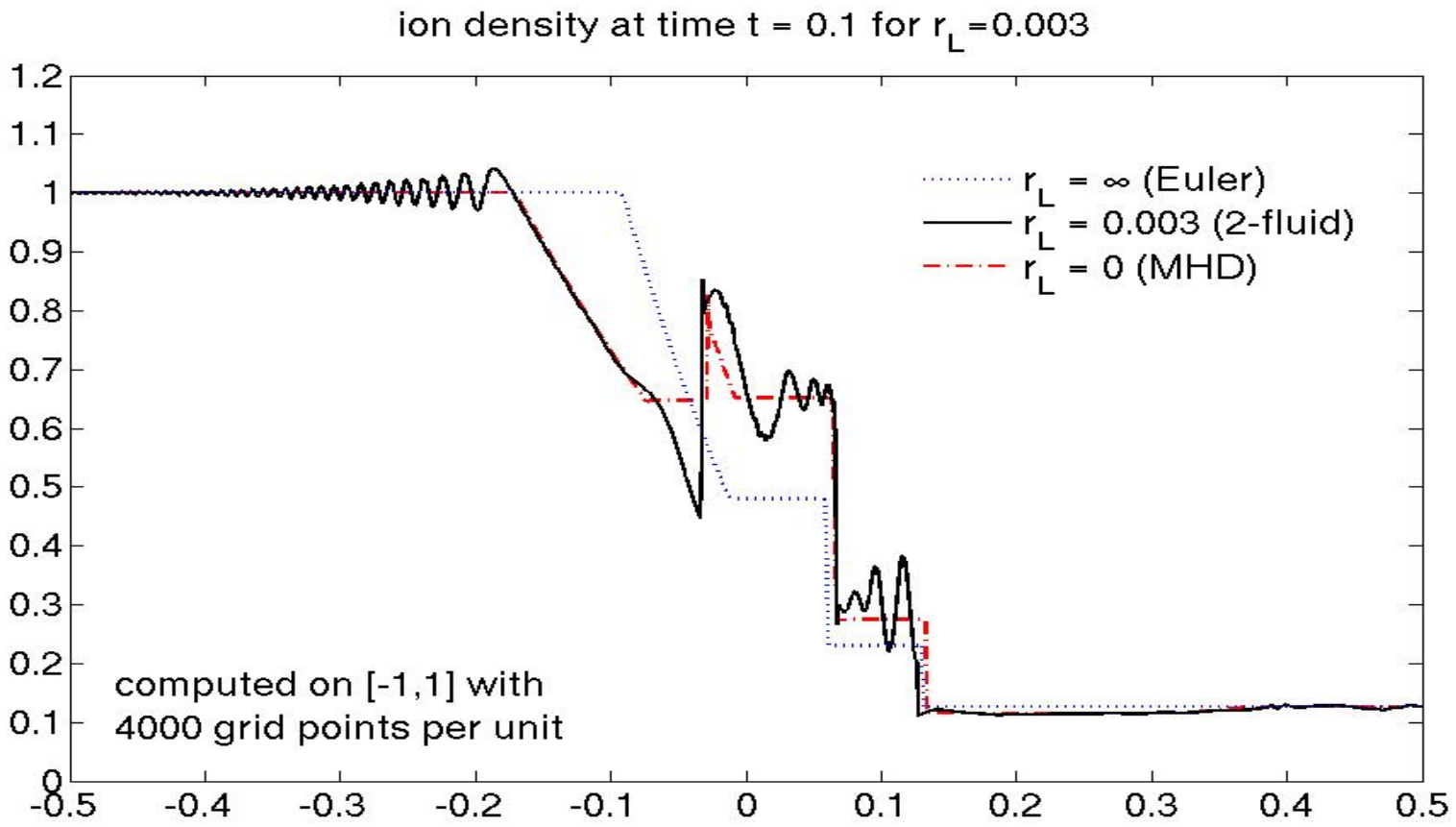

Convergence to MHD is suggested but far from confirmed. Unfortunately, computational expense increases with decreasing Larmor radius.

Acknowledgements

- Wisconsin Space Grant Consortium
- My advisor, James Rossmanith
- Helpful conversations with Nick Murphy, Ping Zhu, Ammar Hakim, Uri Shumlak, James Drake, Nick Hitchon, and Andrew Christlieb.

References

[Birn01] Birn, J., et al., *Geospace Environmental Modeling (GEM) magnetic reconnection challenge*, J. Geophys. Res., 106(A3), 3715–3720, 2001.

[BrioWu88] M. Brio, C. Wu, *An upwind differencing scheme for the equations of magnetohydrodynamics*, Journal of Computational Physics, 75 (1998) 400-422.

[Cockburn97] B. Cockburn, C.-W. Shu, *The Runge-Kutta discontinuous Galerkin method for conservation laws V: multidimensional systems*, Journal of Computational Physics, **141** (1998) 199-224.

[Loverich05] J. Loverich, A. Hakim, U. Shumlak, *A discontinuous Galerkin method for ideal two-fluid plasma equations*, preprint submitted to Journal of Computational Physics, 13 December 2005.

[Hakim06] A. Hakim, J. Loverich, U. Shumlak, *A high resolution wave propagation scheme for ideal two-fluid plasma equations*, Journal of Computational Physics, 219 (2006) 418-442.